Electronic Supplementary Material (ESI) for Journal of Materials Chemistry A.

Supporting Information

Ag, Ti Dual-Cation Substitution in $Cu_2ZnSn(S,Se)_4$ Induced Growth Promotion and Defects Suppression for High-Efficiency Solar Cells

Xing-Ye Chen[a], Muhammad Ishaq[a], Ahmad Nafees[a], Rong Tang[a], Zhuang-Hao Zheng[a], Ju-Guang Hu[a], Zheng-Hua Su[a], Ping Fan[a], Guang-Xing Liang[a,*] and Shuo Chen[a,*]

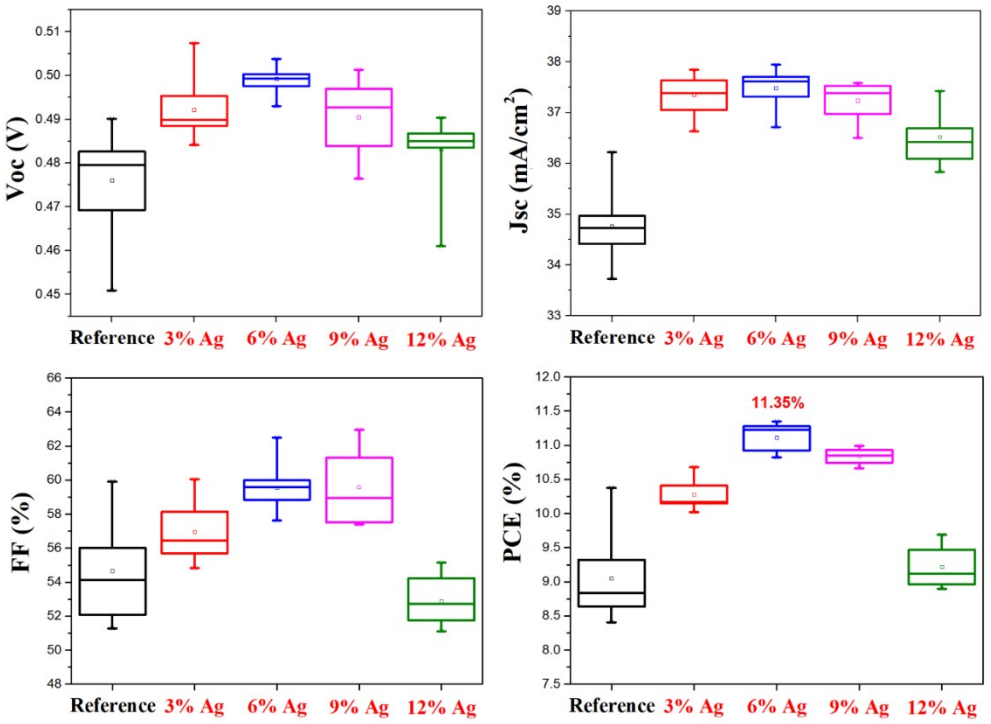

Figure S1. The statistic photovoltaic performances (V_{OC}, J_{SC}, FF and PCE) of CZTSSe-based solar cells with various Ag substitution concentration.

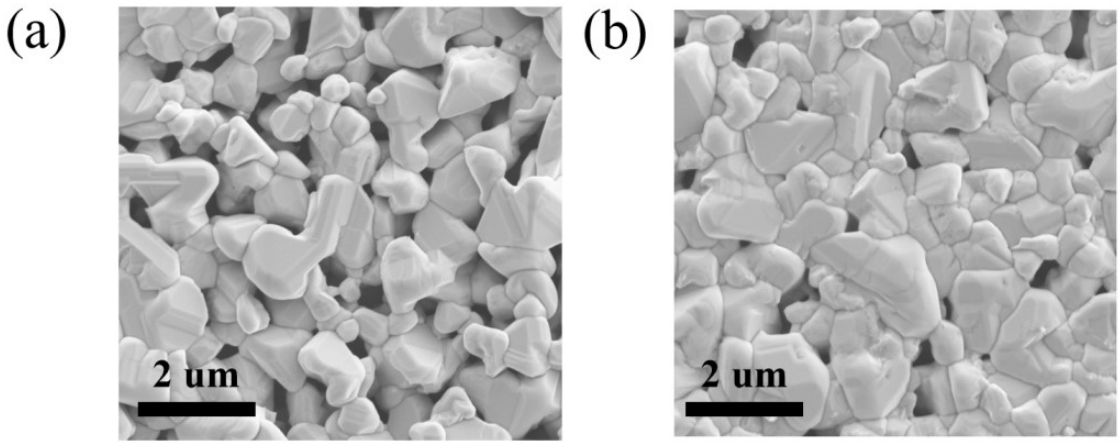

Figure S2. SEM images of (a) Pristine, and (b) Ti substituted CZTSSe thin films.

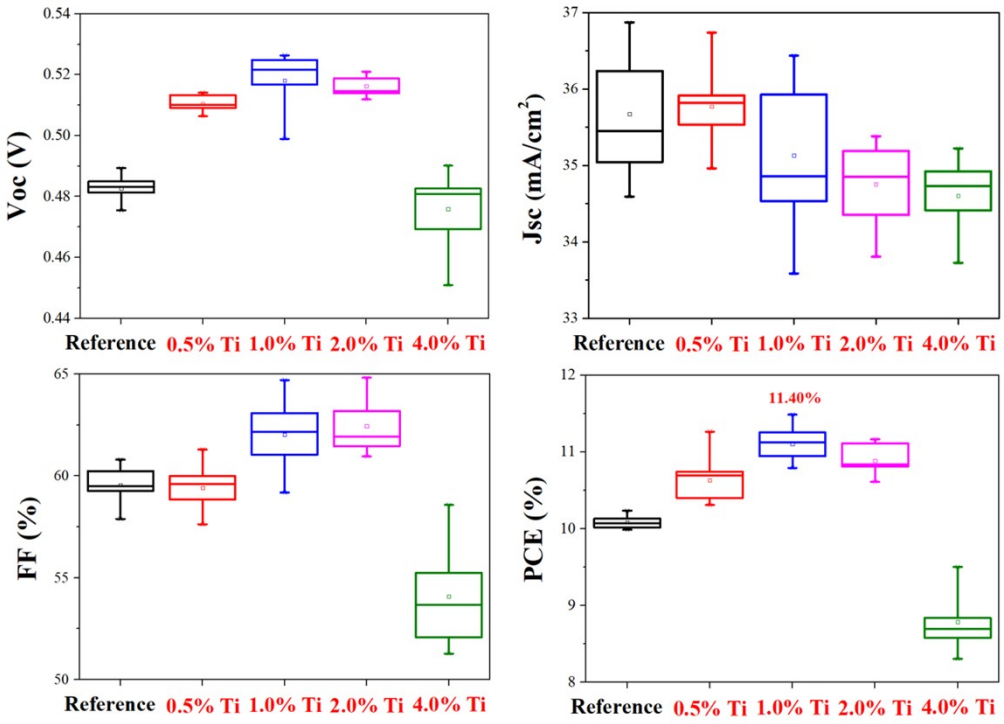

Figure S3. The statistic photovoltaic performances (V_{OC}, J_{SC}, FF and PCE) of CZTSSe-based solar cells with various Ti substitution concentration.

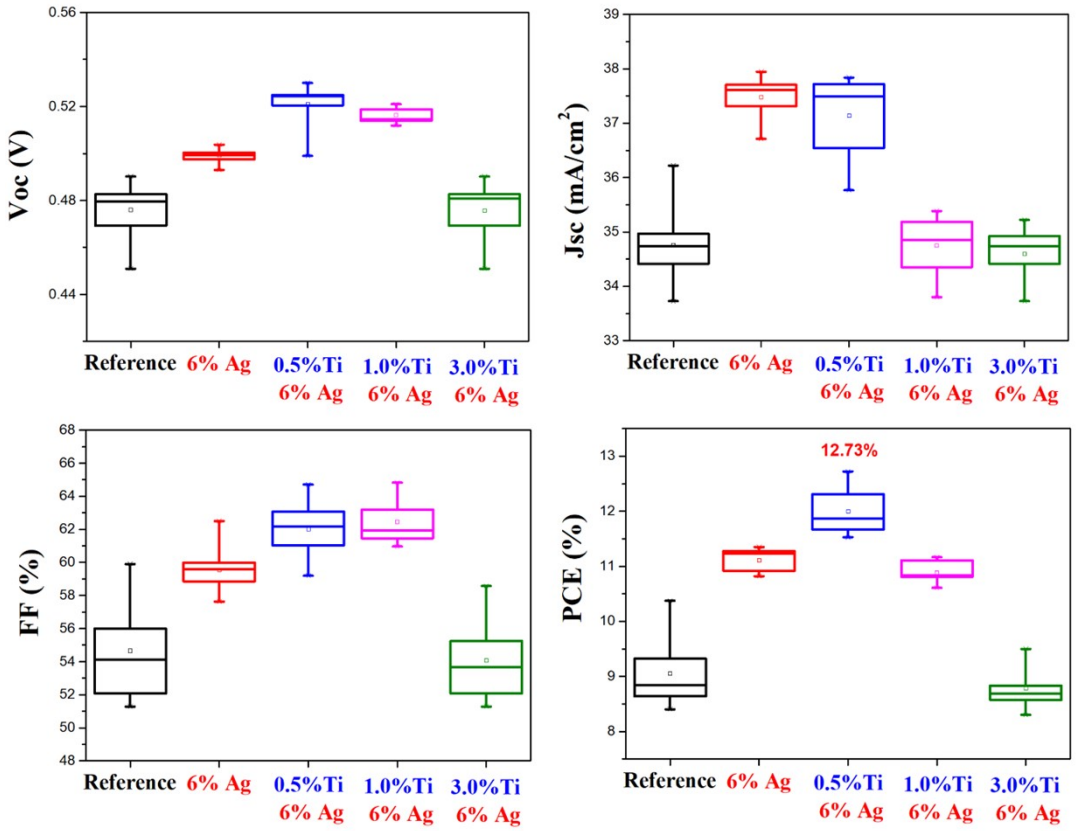

Figure S4. The statistic photovoltaic performances (V_{OC}, J_{SC}, FF and PCE) of 6%-Ag-substituted CZTSSe solar cells and various Ti substitution concentration.

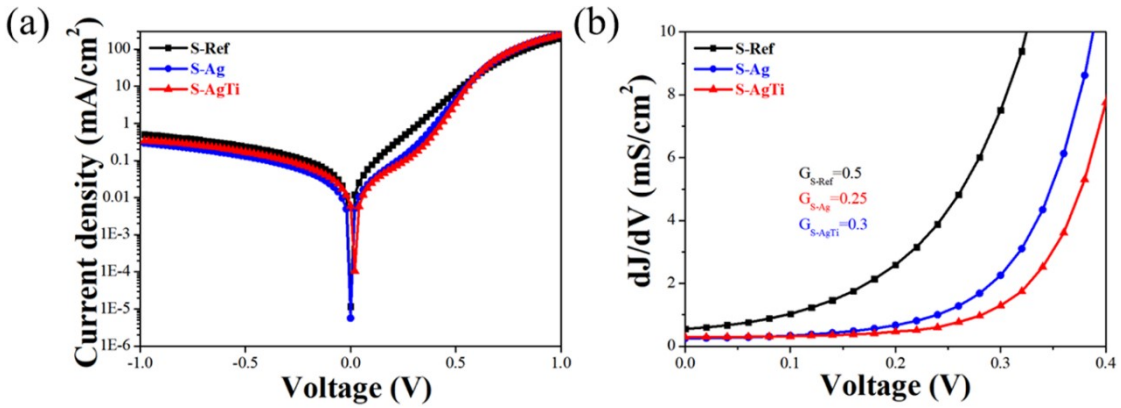

Figure S5. (a) Dark *J-V* curves, and (b) Shunt conductance *G* characterizations of S-Ref, S-Ag and S-AgTi devices.

Table S1. Fitting results of Sn 3d peaks of S-Ref, S-Ag and S-AgTi thin films

Device	Peak intensity ($3d_{5/2}$)			Peak intensity ($3d_{3/2}$)			
	Sn^{4+}	Sn^{2+}	total	Sn^{4+}	Sn^{2+}	Zn-Auger	total
S-Ref	135178	653169	788347	276652	327905	140982	745539
S-Ag	99822	624975	724797	228980	341544	109643	680167
S-AgTi	46474	509831	556305	129929	369864	59379	559172

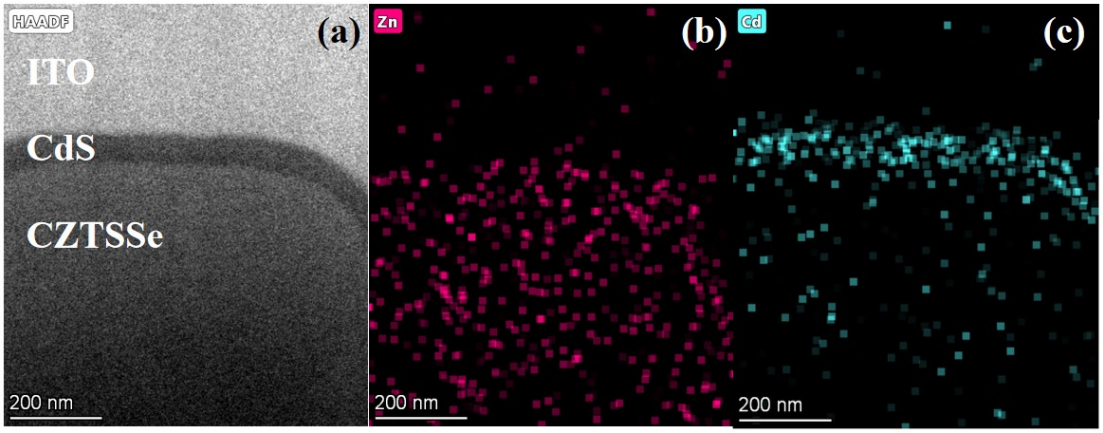

Figure S6. TEM image and TEM-coupled element mapping results for the champion S-AgTi device: (a) Cross-sectional TEM image, (b) Zn, and (c) Cd elemental mapping images.

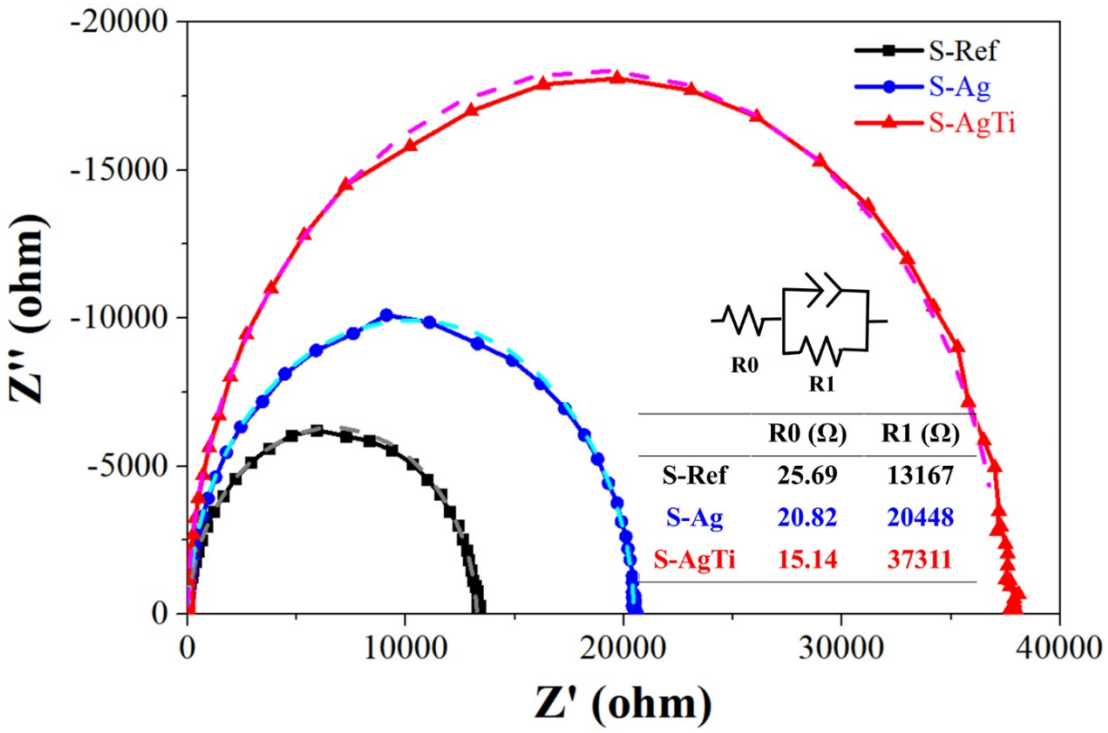

Figure S7. EIS Nyquist plots of S-Ref, S-Ag, and S-AgTi devices. Inset is the equivalent circuit and the corresponding parameters.

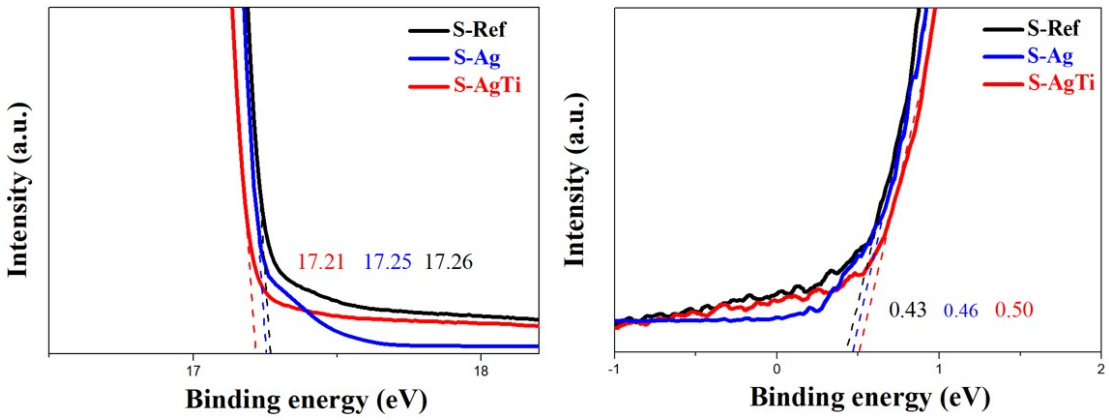

Figure S8. UPS characterizations: secondary electron cut-off (SEC) edge and valence band (VB) position of S-Ref, S-Ag and S-AgTi thin films.